J. Plasma Physics (1999), *vol.* 62, *part* 2, *pp.* 219–232 Printed in the United Kingdom

© 1999 Cambridge University Press

On the evolution of a nonlinear Alfvén pulse

E. VERWICHTE,[1,2] V. M. NAKARIAKOV[1]
and A. W. LONGBOTTOM[1]

[1] School of Mathematical and Computational Sciences, University of St Andrews, St Andrews, Fife KY16 9SS, Scotland
[2] Faculty of Mathematics and Computing, The Open University, Walton Hall, Milton Keynes MK7 6AA, England

(Received 10 November 1998 and in revised form 22 March 1999)

Abstract. The temporal evolution of weakly nonlinear, plane, linearly polarized Alfvén pulses in a cold homogeneous plasma is investigated. A static initial pulse-like disturbance in transverse velocity produces two Alfvén pulses that travel in opposite directions along the magnetic field. The ponderomotive force of the two pulses produces a static shock in longitudinal velocity at the starting position. The travelling pulses form a shock front that is governed by the scalar Cohen–Kulsrud equation. We find good agreement between the analytical solutions we derive and the results from a fully nonlinear numerical MHD code.

1. Introduction

Alfvén and magnetoacoustic waves of finite amplitude are observationally detected in geophysical and astrophysical plasmas; examples include variations of the magnetic field in the solar wind (see e.g. Balogh et al. 1995; Spangler 1997), pulsations in the Earth's magnetosphere (see e.g. Allan and Poulter 1992), low-frequency waves in cometary atmospheres (see e.g. Tsurutani et al. 1987) and fluctuations of physical parameters in the interstellar medium (see e.g. Minter and Spangler 1996). These observations show that the waves reach sufficiently high amplitudes for nonlinear effects to come into play.

It is well known that circularly polarized Alfvén waves of arbitrary amplitude are an exact, although unstable, solution of the full set of ideal magnetohydrodynamic (MHD) equations in the absence of gravity and other external forcing. These waves remain incompressible for any amplitude. In contrast, the behaviour of linearly or elliptically polarized Alfvén waves depends on the wave amplitude. In the linear limit, these waves make the magnetic field and plasma oscillate in the transverse direction with respect to the background magnetic field, and perturb the absolute value of the field. Waves of higher amplitude generate perturbations of plasma density and field-aligned motions, and then interact with the induced perturbations, or 'self-interact'. The self-interaction of the Alfvén waves occurs owing to the action of the ponderomotive force, which is proportional to spatial gradients in the square of the absolute value of the magnetic field.

The weakly nonlinear dynamics of elliptically polarized Alfvén waves is governed by the Cohen–Kulsrud equation (Cohen and Kulsrud 1974). For linearly polarized waves, this equation reduces to the scalar Cohen–Kulsrud (sCK) equation, which is nothing more than a regular simple wave equation

https://doi.org/10.1017/S0022377899007771 Published online by Cambridge University Press

with cubic nonlinearity, possessing an exact analytical solution in an implicit form. The equation describes steepening of the waves, leading to the formation of shocks (current sheets). Consequently, the sCK equation is valid only until the shock appears. In the presence of a smooth inhomogeneity in the Alfvén speed, for example due to gravitational stratification of the plasma density or radial divergence of the magnetic field, the nonlinear dynamics of the Alfvén waves becomes more complicated (see e.g. Boynton and Torkelsson 1996; Torkelsson and Boynton 1998). However, even in this case, the homogeneous theory may give qualitatively correct results is so far as one can neglect the wave reflection from the inhomogeneity, or, in other words, while the WKB approximation is applicable.

The sCK equation describes a wave propagating in one certain direction, and neglects the nonlinear interaction of the wave with other waves, for example backwardly propagating. However, the presence of backwardly propagating waves effects the nonlinear wave dynamics dramatically. In particular, this happens for finite-amplitude Alfvén waves standing in magnetic cavities and Alfvénic resonators. The standing waves can be represented as an interference of two oppositely propagating waves of equal amplitude. Their nonlinear interaction leads to a secular redistribution of plasma along the magnetic field lines and provides a temporally growing non-linear frequency shift of the Alfvén wave (see e.g. Rankin et al. 1994; Tikhonchuk et al. 1995), both of which phenomena are absent from a single-mode model.

In this paper, we investigate another physical situation when nonlinear interaction of two oppositely propagating Alfvén pulses occurs. We consider the development of an initially static plane linearly polarized Alfvén pulse in a homogeneous cold ($\beta = 0$) plasma. The plasma parameter β is defined as the ratio between the kinetic and magnetic pressures of the plasma. The pulse splits into two oppositely propagating pulses. In the initial stage of the splitting, when the pulses have not moved too far away from each other, their back slopes interact nonlinearly, giving rise to a standing shock wave. The shock wave is located at the position of the centre of mass of the two recessive pulses. The formation of the standing shock is found to be a main feature of the initially static Alfvén pulse. Later on, two other shocks are formed on the recessive pulses. We show that the formation of these running shocks can be treated in the single-mode approximation, and is described by the sCK equation. Our analytical weakly nonlinear analysis is supported by fully nonlinear MHD numerical simulations, with good agreement being found between theory and simulations. We employ the non-dissipative Langrangian MHD code from Arber et al. (1999). The code is of second order in space and time. We use a grid resolution $dx = 0.0125 v_A t$. Here we limit our study to the case of a one-dimensional cold plasma.

The paper is organized as follows. In Sec. 2, we describe our model, governing equations and, qualitatively, the scenario of the pulse evolution. In Sec. 3, we present an analytical description of the evolution of the recessive pulses in the single-mode approximation. An analytical theory of the development of the central standing waves is given in Sec. 4. Our results are summarized in Sec. 5.

https://doi.org/10.1017/S0022377899007771 Published online by Cambridge University Press

2. Model

The governing equations are the MHD equation in the zero-β limit. They link the plasma quantities, velocity $\mathbf{v}$ and density ρ, with the magnetic induction $\mathbf{B}$:

$$\frac{\partial \rho}{\partial t} + \boldsymbol{\nabla} \cdot (\rho \mathbf{v}) = 0, \tag{1}$$

$$\rho \left[\frac{\partial}{\partial t} + (\mathbf{v} \cdot \boldsymbol{\nabla}) \right] \mathbf{v} = \frac{1}{\mu_0} (\boldsymbol{\nabla} \times \mathbf{B}) \times \mathbf{B}, \tag{2}$$

$$\frac{\partial \mathbf{B}}{\partial t} = \boldsymbol{\nabla} \times (\mathbf{v} \times \mathbf{B}), \tag{3}$$

$$\boldsymbol{\nabla} \cdot \mathbf{B} = 0, \tag{4}$$

where μ_0 is the magnetic permeability in vacuum.

For the system of equations (1)–(4) a rectangular coordinate system (x, y, z) is chosen. Plane Alfvén pulses, linearly polarized in the z direction, are considered. Therefore variations in the directions perpendicular to the equilibrium magnetic field are assumed to be negligible ($\partial/\partial y = \partial/\partial z = 0$). Perturbations of the plasma and the magnetic field in the z direction are taken into account, but those in the y direction are assumed to be zero.

The MHD equations are studied in the weakly nonlinear regime. Consider small but finite perturbations around a static equilibrium comprising a uniform density ρ_0 and a uniform magnetic field $B_0 \, \mathbf{1}_x$ (e.g. $\rho = \rho_0 + \epsilon \rho'$). The expansion parameter ϵ ($0 < \epsilon < 1$) is proportional to the dimensionless amplitude a of the linear solution. Thus (1)–(4) reduce to

$$\frac{\partial \rho'}{\partial t} + \rho_0 \frac{\partial v_x'}{\partial x} = -\frac{\partial}{\partial x} (\rho' v_x'), \tag{5}$$

$$\rho_0 \frac{\partial v_x'}{\partial t} = -\frac{1}{2\mu_0} \frac{\partial B_z'^2}{\partial x} - \rho \frac{\partial v_x'}{\partial t} - \rho_0 v_x' \frac{\partial v_x'}{\partial x} - \rho v_x' \frac{\partial v_x'}{\partial x}, \tag{6}$$

$$\rho_0 \frac{\partial v_z'}{\partial t} - \frac{B_0}{\mu_0} \frac{\partial B_z'}{\partial x} = -\rho \frac{\partial v_z'}{\partial t} - \rho_0 v_x' \frac{\partial v_z'}{\partial x} - \rho v_x' \frac{\partial v_z'}{\partial x}, \tag{7}$$

$$\frac{\partial B_x'}{\partial t} = 0, \tag{8}$$

$$\frac{\partial B_z'}{\partial t} - B_0 \frac{\partial v_z'}{\partial x} = -\frac{\partial}{\partial x} (v_z' B_z'). \tag{9}$$

The prime denoting perturbed quantities will be omitted from now on to simplify the notation. The purely linear terms are gathered on the left-hand sides and all the nonlinear terms are gathered on the right-hand sides. Equation (8) reveals that there are no magnetic field perturbations in the longitudinal direction (x direction).

https://doi.org/10.1017/S0022377899007771 Published online by Cambridge University Press

The perturbation quantities are expanded in powers of the parameter ϵ (e.g. $\rho' = \rho_1 + \epsilon\rho_2 + \ldots$). The subscript denotes the order of the quantity. We introduce two independent time scales $t_0 = t$ and $\tau = \epsilon^2 t$ so that

$$\frac{\partial}{\partial t} = \frac{\partial}{\partial t_0} + \epsilon^2 \frac{\partial}{\partial \tau} \tag{10}$$

The time scale τ is slow compared with t_0. It is proportional to a^2. Hence any non-zero term in (5)–(9) containing the time scale τ is of at least third order. For clarity in notation, the subscript 0 on the first time scale will be omitted.

The first-order linearizations of (7) and (9) combine into an Alfvén-wave equation:

$$\left(\frac{\partial^2}{\partial t^2} - V_A^2 \frac{\partial^2}{\partial x^2}\right) B_{z,1} = 0, \tag{11}$$

with the quantity $V_A = B_0(\rho_0 \mu_0)^{-1/2}$ being the background Alfvén speed. Since there are no boundary conditions in x, the solution to (11) is expressed as the d'Alembert solution, $B_{z,1} = aB_0[f(x + V_A t) + g(x - V_A t)]$, describing two waves, one travelling in the positive and the other in the negative x direction, both at the background Alfvén speed. The shapes of the functions f and g are determined by the initial conditions $B_{z,1}(t\,0)$ and $(\partial B_{z,1}/\partial t)\,(t = 0)$. We consider the solution excited by an initial pulse in the velocity ($B_{z,1}(t = 0) = 0$, $v_{z,1}(t = 0) = 2aV_A \mathscr{F}(x), \xi_{z,1}(t = 0) = 0$):

$$\frac{B_{z,1}}{B_0} = a[\mathscr{F}(x + V_A t, \tau) - \mathscr{F}(x - V_A t, \tau)]. \tag{12}$$

Throughout this paper, both numerical and analytical results are illustrated by taking the function $\mathscr{F}(s)$ to have the form of a Gaussian pulse

$$\mathscr{F}(s) = e^{-(s/\Delta x)^2}, \tag{13}$$

which is localized at $s = 0$ ($\mathscr{F}(0) = 1$) and has a spatial width Δx, with monotonically decaying wings that tail off to zero as s tends to infinity.

If there are no initial perturbations of the longitudinal velocity or the density, the only term that can excite them is the first term on the right-hand side of (6), which is the nonlinear Alfvén magnetic pressure force (the second-order ponderomotive force). It is of order a^2. Therefore the quantities v_z and ρ are of order a^2 as well. Using the linear solution (12), the second-order ponderomotive force is

$$\begin{aligned} -\frac{1}{2\mu_0}\frac{\partial B_{z,1}^2}{\partial x} = & -\frac{1}{2}\rho_0 a^2 V_A^2 \frac{\partial}{\partial x}[\mathscr{F}^2(x + V_A t) + \mathscr{F}^2(x - V_A t) \\ & - 2\mathscr{F}(x + V_A t)\,\mathscr{F}(x - V_A t)]. \end{aligned} \tag{14}$$

The ponderomotive force is the only force, besides the inertia of the plasma, that is directed along the equilibrium magnetic field. In the case considered, it consists of three terms. The first two are, at every time, localized at the position of the pulses. We call them the 'ponderomotive wings'. At a fixed position through which a pulse passes, the flow induced by the ponderomotive force of the preceding flank of the pulse is counteracted by the flow induced by the

https://doi.org/10.1017/S0022377899007771 Published online by Cambridge University Press

ponderomotive force of the following flank. The ponderomotive response to these force terms will always remain of order a^2. The third term is the cross-term of the two pulses, localized at $x = 0$ and decreasing in magnitude rapidly in time with a time scale $\Delta x/V_A$ as the two Alfvén pulses separate. We call this term the 'cross-ponderomotive force'. In a cold, ideal plasma, there is no force decelerating the flow of the plasma excited by this cross-ponderomotive force. Therefore we expect locally large density perturbations to occur in time. Figure 1 gives from a numerical simulation a general view of the spatial structure of the quantities v_z, v_x and ρ at three time steps.

The above comments are illustrated by the solution to (5) and (6) at second order,

$$\frac{\partial \rho_2}{\partial t} = -\rho_0 \frac{\partial v_{x,2}}{\partial x}, \tag{15}$$

$$\rho_0 \frac{\partial v_{x,2}}{\partial t} = -\frac{1}{2\mu_0} \frac{\partial B_{z,1}^2}{\partial x}, \tag{16}$$

which are, in the case of Gaussian-shaped pulses,

$$\frac{\rho_2}{\rho_0} = \frac{1}{2}a^2 \Bigg\{ \mathscr{F}^2(x + V_A t) + \mathscr{F}^2(x - V_A t) - 2\mathscr{F}^2(x) + 2\pi^{1/2} \left[1 - 4\left(\frac{x}{\Delta x}\right)^2 \right] e^{-2(x/\Delta x)^2} \int_0^{\sqrt{2}V_A t/\Delta x} \operatorname{erf}(t')\, dt' \Bigg\}, \tag{17a}$$

$$\frac{v_{x,2}}{V_A} = -\frac{1}{2}a^2 \Bigg[\mathscr{F}^2(x + V_A t) - \mathscr{F}^2(x - V_A t) + 2(2\pi)^{1/2} \frac{x}{\Delta x} e^{-2(x/\Delta x)^2} \operatorname{erf}\left(\sqrt{2} \frac{V_A}{\Delta x} t \right) \Bigg]. \tag{17b}$$

The last terms in the expressions for $v_{x,2}$ and ρ_2 represent the response to the cross-ponderomotive force. The time profile of the velocity, due to this force, is that of an error function. After a time of approximately $\Delta x/\sqrt{2}V_A$, the velocity is constant, with the spatial structure of an inward flow towards $x/\Delta x = 0$. At $x/\Delta x = \pm 1/2$, the velocity has a local extremum. The density at $x/\Delta x = 0$ has a maximum in space. At first, the density grows quadratically, but after a time of approximately $\Delta x/\sqrt{2}V_A$, the growth becomes linear. Figure 2 shows both the spatial structure at the time $V_A t/\Delta x = 0.63$ and the early time evolution of the numerically derived quantities v_x and ρ, compared with the quadratically nonlinear solution (17). The quadratically nonlinear solution matches the numerical result very well up to a time $V_A t/\Delta x \approx 2$. Beyond that time, other nonlinear processes become important.

At first, all three terms in (14) are of the same magnitude. The cross-ponderomotive force, however, decreases exponentially with time, and eventually becomes one order of magnitude less than the force of the ponderomotive wings. We estimate the time t_{sep} at which this occurs:

$$\left| \frac{\mathscr{F}^2(x \pm V_A t_{\text{sep}})}{2\mathscr{F}(x + V_A t_{\text{sep}})\, \mathscr{F}(x - V_A t_{\text{sep}})} \right| \approx 10. \tag{18}$$

https://doi.org/10.1017/S0022377899007771 Published online by Cambridge University Press

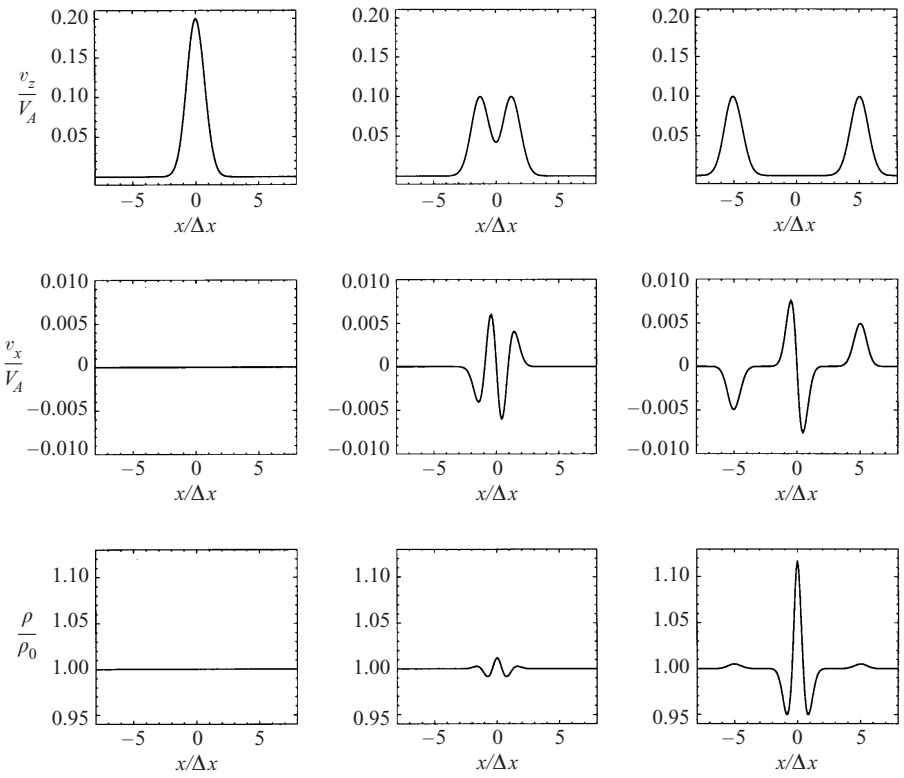


Figure 1. A numerical simulation of Alfvén pulses in the transverse velocity v_z and the ponderomotive response in longitudinal velocity v_x and density ρ as functions of x at times $V_A t/\Delta x = 0$, 1.25 and 5. The amplitude parameter $a = 0.1$.

In the case of Gaussian-shaped pulses, the time $t_{\rm sep}$ is given by

$$\frac{V_A t_{\rm sep}}{\Delta x} \approx \sqrt{0.5 \ln 20} \approx 1.22. \tag{19}$$

The solution (17) remains of order a^2 for times earlier than $t_{\rm sep}$ when

$$\frac{\rho_2}{\rho_0} \ll \frac{B_{z,1}}{B_0}, \tag{20}$$

which, in the case of Gaussian-shaped pulses, yields the condition

$$a \ll \left[\pi^{1/2} \int_0^{\sqrt{2} V_A t_{\rm sep}/\Delta x} \mathrm{erf}(t')\, dt' \right]^{-1} \approx 0.48. \tag{21}$$

For amplitudes that satisfy the condition (20), the ponderomotive response is of order a^2 for times earlier than $t_{\rm sep}$. After $t_{\rm sep}$, the ponderomotive response to the three terms of the ponderomotive force (14) can be treated separately. This implies that the full solution is built up by three treatments. First, the solution at times earlier than $t_{\rm sep}$ is adequately described by the linear and quadratic nonlinear solutions (12) and (17). For times later than $t_{\rm sep}$, we treat the nonlinear behaviour of the Alfvén wings and the central part separately. This is the central idea of the model.

https://doi.org/10.1017/S0022377899007771 Published online by Cambridge University Press

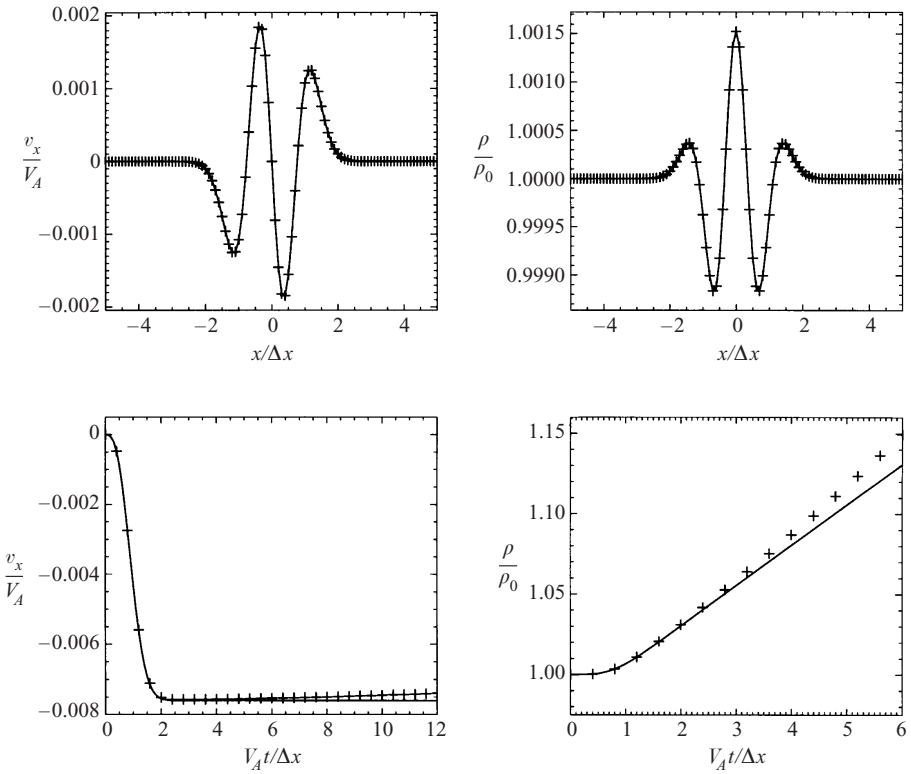


Figure 2. Plots of the longitudinal velocity v_x and density ρ. The top panels show the spatial behaviour at an early time $V_A t/\Delta x = 0.63$. The bottom panels show the early time evolution of the velocity v_x at $x/\Delta x = 0.5$ and the density ρ at $x/\Delta x = 0$. The crosses are the full numerical result. The solid line is the quadratically nonlinear solution (17). The amplitude parameter $a = 0.1$.

The terms on the right-hand sides of (7) and (9) contain the nonlinear corrections to the Alfvén pulses. They are of order a^3, and consist of a combination of the perturbations governing the Alfvén pulses and their ponderomotive response. These corrections appear in the ponderomotive force as terms of order a^4.

The Alfvén correction terms that contain the ponderomotive response of the cross-ponderomotive force are expected to grow in magnitude for times earlier than $t_{\rm step}$, but after that decrease exponentially to zero. The maximum magnitude of these terms is negligible under the condition (20). Thus, for the treatment of the central region, the nonlinear terms in (7) and (9) are neglected, even though we keep the terms of order a^4 in (5) and (6). Moreover, the terms proportional to the perturbed density ρ in (6) are neglected as well. This is because, before time $t_{\rm sep}$, the terms proportional to ρ are negligible because $\rho \ll \rho_0$. After time $t_{\rm sep}$, the cross-ponderomotive force is negligible, and the density $\rho_0 + \rho$ is eliminated from the remaining equation.

For the ponderomotive wings, it is not possible to neglect the nonlinear Alfvén correction terms a^3 without neglecting the terms of order a^4 in (5) and (6) as well. Therefore we shall investigate the effect of these nonlinear Alfvén correction terms by looking at the self-modification of a finite-amplitude Alfvén pulse.

https://doi.org/10.1017/S0022377899007771 Published online by Cambridge University Press

3. Self-modification of Alfvén pulses

In this section, we shall address the self-modification of a travelling Alfvén pulse of finite amplitude. This is a cubic nonlinear effect. Instead of the first-order solution (12), we take only one pulse:

$$\frac{B_{z,1}}{B_0} = a\mathscr{F}(x \pm V_A t, \tau). \tag{22}$$

The second-order solutions are easily obtained by looking at the expressions (17):

$$\frac{\rho_2}{\rho_0} = \frac{1}{2}\left(\frac{B_{z,1}}{B_0}\right)^2, \tag{23}$$

$$\frac{v_{x,2}}{V_A} = \mp\frac{1}{2}\left(\frac{B_{z,1}}{B_0}\right)^2. \tag{24}$$

The third-order equations, using the previous results (22)–(24), are

$$\rho_0\frac{\partial v_{z,3}}{\partial t} - \frac{B_0}{\mu_0}\frac{\partial B_{z,3}}{\partial x} = -\rho_0\frac{\partial v_{z,1}}{\partial \tau}, \tag{25}$$

$$\frac{\partial B_{z,3}}{\partial t} - B_0\frac{\partial v_{z,3}}{\partial x} = -\frac{\partial B_{z,1}}{\partial \tau} - \frac{\partial}{\partial x}(v_{x,2}B_{z,1}). \tag{26}$$

Eliminating the secular terms yields a quasilinear equation in the magnetic field perturbation $B_{z,1}$:

$$\frac{\partial B_{z,1}}{\partial \tau} \mp \frac{3}{4}V_A\left(\frac{B_{z,1}}{B_0}\right)^2\frac{\partial B_{z,1}}{\partial x} = 0, \tag{27}$$

which is known as the Cohen–Kulsrud equation (Cohen and Kulsrud 1974). Its solution is

$$\frac{B_{z,1}}{B_0} = a\mathscr{F}\left(x \pm V_A t \pm \frac{3}{4}V_A\left(\frac{B_{z,1}}{B_0}\right)^2\tau\right). \tag{28}$$

Since the propagation speed of the function $\mathscr{F}$ now depends on the square of the function itself, we have the possibility of shock formation, because the centre of the pulse moves faster than the preceding wing of the pulse, thus catching up with the preceding wing (see Fig. 3). A shock is formed when locally the time and space derivatives become infinite.

Assuming that the function $\mathscr{F}$ has an inverse, we take the spatial derivative of that inverse function $\mathscr{F}^{-1}(B_{z,1})$:

$$\frac{1}{B_0}\frac{d\mathscr{F}^{-1}}{dB_{z,1}}\frac{\partial}{\partial x}\left(\frac{B_{z,1}}{B_0}\right) = 1 \pm \frac{3}{2}V_A\frac{B_{z,1}}{B_0}\frac{\partial}{\partial x}\left(\frac{B_{z,1}}{B_0}\right)\tau, \tag{29}$$

which at $\tau = 0$ yields

$$\frac{1}{B_0}\frac{d\mathscr{F}^{-1}}{dB_{z,1}} = \left[\frac{\partial}{\partial x}\left(\frac{B_{z,1}}{B_0}\right)\right]^{-1}_{\tau=0}. \tag{30}$$

https://doi.org/10.1017/S0022377899007771 Published online by Cambridge University Press

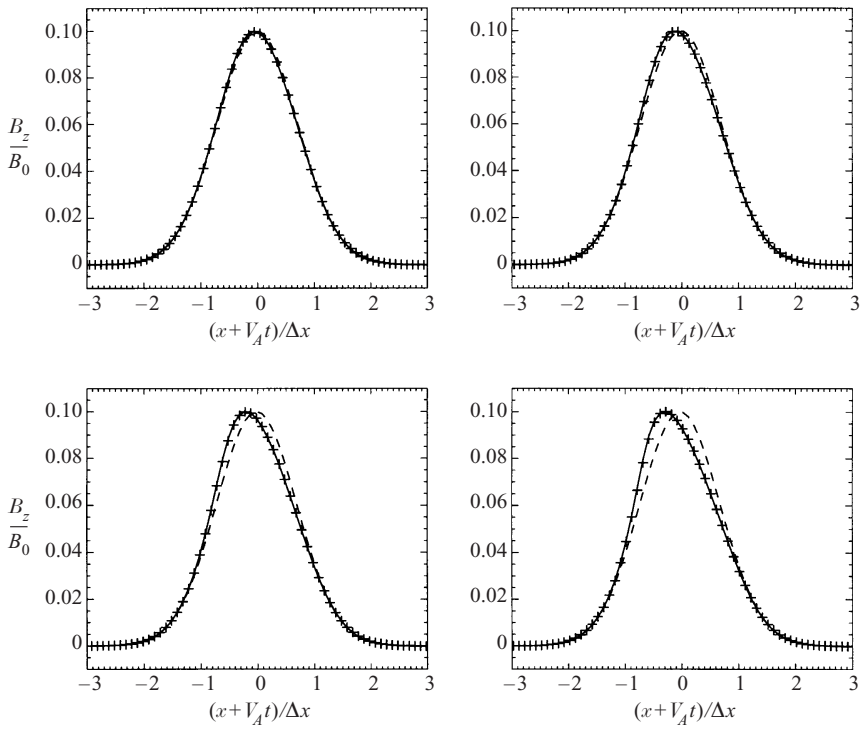


Figure 3. Plots of the magnetic perturbation B_z of the Alfvén pulse travelling in the negative x direction as a function of $x+V_A t$ at different times $V_A t/\Delta x = 6.3$, 13.8, 25.0 and 36.3. The crosses are the full numerical result. The solid line is the expression (28). The dashed line is the linear expression (12). The amplitude parameter $a = 0.1$.

Eliminating the x derivative of the magnetic field perturbation $B_{z,1}$ from (29) and using the previous expression, we find

$$\frac{\partial}{\partial x}\left(\frac{B_{z,1}}{B_0}\right) = \frac{\dfrac{\partial}{\partial x}\left(\dfrac{B_{z,1}}{B_0}\right)_{\tau=0}}{1 \mp \dfrac{3}{2} V_A \dfrac{B_{z,1}}{B_0} \dfrac{\partial}{\partial x}\left(\dfrac{B_{z,1}}{B_0}\right)_{\tau=0} \tau}. \tag{31}$$

The earliest time (say τ_{sw}) at which the x derivative of the magnetic field perturbation is infinite, thus forming a shock, is

$$\tau_{sw} = \min\left\{ \pm \frac{1}{\dfrac{3}{4} V_A a^2 \left[\dfrac{\partial}{\partial x}\left(\dfrac{B_{z,1}}{B_0}\right)^2\right]_{\tau=0}} \right\}. \tag{32}$$

The magnetic field perturbation $B_{z,1}$ in the denominator of (31) has been approximated by its initial profile at $\tau = 0$. The magnetic field perturbation and its spatial derivative need to have the same sign somewhere in the spatial domain in order to have the possibility of shock formation. The time scale for shock formation is inversely proportional to a^2. With the function $\mathscr{F}$ defined as (13), the shock forms at the time $V_A \tau_{sw}/\Delta x = 2e^{1/2}/3a^{-2} \approx 1.1a^{-2}$ at the position $(x \pm V_A t)/\Delta x = \mp 1$.

https://doi.org/10.1017/S0022377899007771 Published online by Cambridge University Press

4. Cross-ponderomotive force

With the assumptions made in Sec. 2, the equations to be solved for the cross-ponderomotive force are

$$\frac{\partial \rho}{\partial t}+\frac{\partial}{\partial x}(\rho v_x)=0, \tag{33}$$

$$\frac{\partial v_x}{\partial t}+v_x\frac{\partial v_x}{\partial x}=a^2V_A^2\frac{\partial}{\partial x}[\mathscr{F}(x+V_At)\,\mathscr{F}(x-V_At)]. \tag{34}$$

The momentum equation is decoupled from the mass-conservation equation. The difference between (16) and (34) is the inclusion of the inertial term on the left-hand side. The force term on the right-hand side of (34) is rapidly decreasing to zero on the fast time scale $V_At/\Delta x$.

First of all, we assume that the time scale of the cross-ponderomotive force is faster than the time scale of the nonlinear inertial term $v_x\,\partial v_x/\partial x$ in (34). For times $t<t_{\rm sep}$, the solution for v_x is given as

$$v_{x,c}=a^2V_A^2\int_0^t dt'\frac{\partial}{\partial x}[\mathscr{F}(x+V_At')\,\mathscr{F}(x-V_At')]. \tag{35}$$

In the case of Gaussian-shaped pulses, this corresponds to the last term of (17b). From the time $t_{\rm sep}$ onwards, the velocity is approximately time-independent because the force term has become negligible. We therefore switch off the force term and switch on the nonlinear inertial term. We feed the solution (35), evaluated at t tending to infinity, $\bar{v}_x=v_{x,c}(t=\infty)$, as an initial condition at $t=t_{\rm sep}$ into the simple wave equation $\partial v_x/\partial t+v_x\,\partial v_x/\partial x=0$. The characteristic equation is then

$$\frac{dx(t)}{dt}\approx\bar{v}_x. \tag{36}$$

The velocity $v_{x,c}$ is constant along the characteristic, which is a straight line. The solution of (36) is then

$$x(t)=x(t_{\rm sep})+\bar{v}_xt. \tag{37}$$

When for the first time (say at time t_{sc}) two neighbouring characteristics intersect (this corresponds to the condition that a gradient becomes infinite), a surface of discontinuity has formed:

$$x^{(+)}(t_{sc})=x^{(-)}(t_{sc})\quad\text{when}\quad\frac{V_At_{sc}}{\Delta x}=\min\left\{\frac{1}{\dfrac{\partial\bar{v}_x}{\partial x(t_{\rm sep})}}\right\}. \tag{38}$$

In case of Gaussian-shaped pulses, this becomes

$$\frac{V_At_{sc}}{\Delta t}=\min\left\{\frac{1}{(2\pi)^{1/2}a^2\dfrac{\partial}{\partial\xi}(\xi e^{-2\xi^2})}\right\}=\frac{1}{(2\pi)^{1/2}a^2}. \tag{39}$$

The surface of discontinuity forms at the position $x=0$, where the original Alfvén-pulse disturbance was centred at $t=0$.

https://doi.org/10.1017/S0022377899007771 Published online by Cambridge University Press

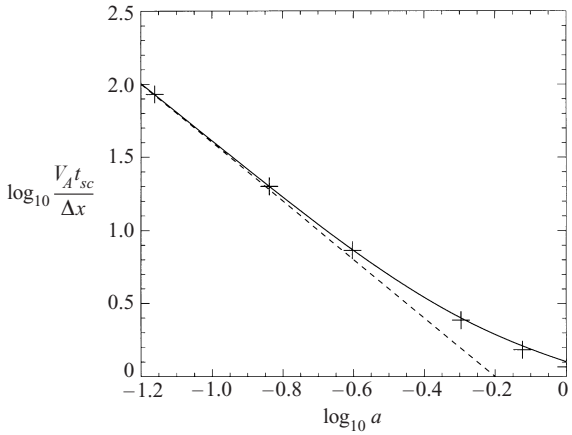


Figure 4. A logarithmic plot of the dependence of the time t_{sc} for the formation of the surface of discontinuity on the amplitude parameter a. The crosses show the full numerical result. The solid line is the numerically derived solution of (40). The dashed line shows the analytical result (39).

From (39), we conclude that the time scale for the formation of the surface of discontinuity is inversely proportion to a^2. Figure 4 shows the time t_{sc} deduced both analytically and numerically. The result deduced using the one-dimensional MHD Lagrangian code is the most accurate, since it assumes nothing besides the one-dimensionality of the problem. The analytical result matches the other results very well for small values of the parameter a, but starts to diverge once $a > 0.2$, reaching the limitation (20). For larger values of a, the time scales for the cross-ponderomotive force and the inertia become comparable. The two terms counteract each other at times earlier than t_{sep}. This means that the second-order solution (17) does not approximate the full solution well enough. This is reflected by the fact that the shock formation time is no longer proportional to a^{-2} but is more like a^{-4}. After the time t_{sep}, the inertia dominates, driving the velocity to a shock. The solid curve in Fig. 4 takes into account the competition between the ponderomotive force and inertia, since it is the numerical solution of the forced simple wave equation

$$\frac{\partial v_x}{\partial t} + v_x \frac{\partial v_x}{\partial x} = -\frac{1}{2\mu_0 \rho_0} \frac{\partial B_{z,1}^2}{\partial x}, \tag{40}$$

assuming that the magnetic perturbation $B_{z,1}$ is given by (12). The full ponderomotive force (14) is considered, but we only focus on its effect on the relevant central region. Figure 5 shows plots of the velocity v_x, derived using the previous equation, as a function of x for several times. The steepening of the gradient with time at $x = 0$ is clearly visible. Up to $a = 0.6$, this result matches very well with the full numerical result. The deviation between the two results for higher values of a is due to the neglect of the self-modification of the Alfvén pulses. For these values of a, the Alfvén pulses modify themselves substantially before they separate ($t < t_{\text{sep}}$), thus affecting the ponderomotive response in the central region after all. On top of that, the amplitude a becomes of order 1, violating the perturbation approach. We therefore expect in this regime deviations between the analytical solutions and the numerical results anyway.

https://doi.org/10.1017/S0022377899007771 Published online by Cambridge University Press

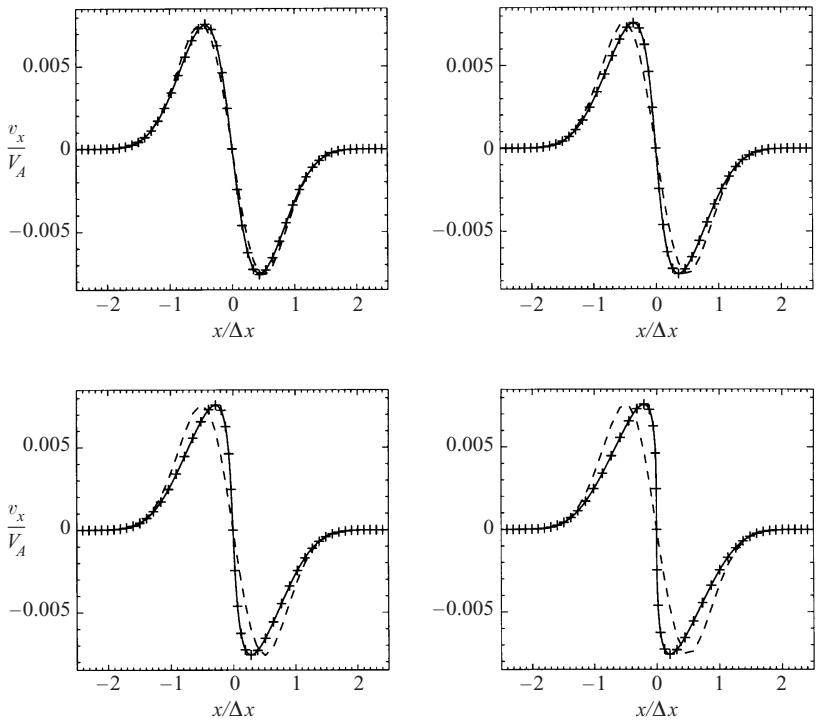


Figure 5. Plots of the velocity perturbation v_x as a function of x at different times $V_A t/\Delta x = 10.0$, 20.0, 30.0 and 39.9. The last time corresponds to the time t_{se}. The crosses are the full numerical result. The solid line is the numerical solution to (40). The dashed line is the quadratically nonlinear solution $v_{x,2}$. The amplitude parameter $a = 0.1$.

5. Discussion

This paper has put forward a model for describing the weakly nonlinear behaviour of finite-amplitude Alfvén pulses, linearly polarized in the z direction. Variations in the directions perpendicular to the background magnetic field direction are neglected. Perturbations of the plasma and the magnetic field in the z-direction are taken into account and those in the y direction are taken to be zero. When initially a pulse in the transverse velocity or displacement is excited, two Alfvén pulses are created, which travel in opposite directions along the background magnetic field. The ponderomotive force that is associated with this magnetic disturbance excites longitudinal plasma flows and density perturbations. It has three contributions: the first two terms contain only the magnetic perturbation of either the pulse travelling in the positive direction or of the pulse travelling in the negative direction (ponderomotive wings). The third term consists of a combination of the magnetic perturbation of both pulses (the cross-ponderomotive force). It decreases rapidly to zero as the two pulses separate. We have defined a time $t_{\rm sep}$ at which the cross-ponderomotive force has become at least one order of magnitude smaller than the ponderomotive wings. From this, we have found an upper limit for the amplitude parameter a for which the perturbed density remains of order a^2 for times earlier than $t_{\rm sep}$. Within this limit, the problem is split up into three parts. The initial behaviour ($t < t_{\rm sep}$) is represented well by the quadratically nonlinear

https://doi.org/10.1017/S0022377899007771 Published online by Cambridge University Press

solution. After that time, the nonlinear evolution of the wings and the central part can be treated separately.

For the wings, we have found that the shape of the Alfvén pulse is governed by the scalar Cohen–Kulsrud equation. The preceding side of the Alfvén pulse steepens into a shock front on a time scale that is inversely proportional to a^2. shocks are effective in converting hydromagnetic wave energy into heat. Cohen and Kulsrud (1974) showed that in a warm plasma the rate of heating per unit volume, dQ/dt, is given by

$$\frac{dQ}{dt} = \frac{1}{8}\frac{\rho_0 V_A^3}{L(1-\beta)B_0^4}(B_{zp}^2 - B_{zf}^2)(B_{zp} - B_{zf})^2, \tag{41}$$

where L is the typical length scale that covers a spatial interval where only one shock is present, and B_{zp} and B_{zf} are the z components of the magnetic field perturbations on the preceding and following sides respectively.

In the central region, the excited plasma flow profile is such that it pushes mass together at the position $x/\Delta x = 0$. The nonlinear evolution of this flow profile is represented well by the solution of the forced simple wave equation (40), which we have solved numerically using the method of characteristics. The profile forms a surface discontinuity in the flow velocity on a time scale that is proportional to a^2. This central shock develops well before the propagating shocks. At the position $x/\Delta x = 0$, the density becomes infinite. In reality, this cannot occur. Eventually, the kinetic pressure and viscosity – no matter how small they might be – will counteract the build-up of the large gradients in the flow velocity. It is therefore a necessary next step to include the plasma pressure in the calculations.

For values of the amplitude parameter a that are close to or exceed the upper limit (20), our model becomes inadequate, mainly because the Alfvén pulses are modified by the ponderomotive response of the other pulse and the cross-ponderomotive response. Those terms were neglected on the right-hand sides of (7) and (9). To account for these terms, a more general evolutionary equation is needed.

In this paper, we have looked at a pulse that was excited in the transverse velocity component v_z. An Alfvén pulse can, of course, also be excited in the transverse displacement component ξ_z ($B_{z,1}(t=0) = 2aB_0 L\,\partial\mathscr{F}(x)/\partial x$, $v_{z,1}(t=0) = 0$, $\xi_{z,1}(t=0) = 2aL\,\mathscr{F}(x)$) or in the transverse magnetic field component B_z($B_{z,1}(t=0) = 2aB_0\,\mathscr{F}(x)$, $v_{z,1}(t=0) = 0$, $\xi_{z,1}(t=0) = 2a\int dx\,\mathscr{F}(x)$). It can be seen that the former case is very similar to the case that we have considered here, because the cross-ponderomotive force in this case has the same sign. The shape of the pulse is now a spatial derivative of the pulse shape, but we still see mass accumulating at $x = 0$. The latter case, however, is different, because the cross-ponderomotive force has the opposite sign to the case that we have considered. The quadratically nonlinear solution to this problem is given by the expressions (17a,b), with opposite signs for the last term in each equation. Consequently, mass is now pushed out of the region around $x/\Delta x = 0$. Also, the expression (35) differs only in sign. Therefore (39) becomes

$$\frac{V_A t_{sc}}{\Delta x} = \min\left\{\frac{-1}{(2\pi)^{1/2}a^2\dfrac{\partial}{\partial\xi}(\xi e^{-2\xi^2})}\right\} = \frac{1}{2e^{-3/2}(2\pi)^{1/2}a^2}. \tag{42}$$

https://doi.org/10.1017/S0022377899007771 Published online by Cambridge University Press

A surface discontinuity appears at the positions $x/\Delta x = \pm\frac{1}{2}\sqrt{3}$. The latter case is unphysical, however, because it starts out with an excited displacement ξ_z that does not tail off to zero as x tends to infinity. It is relevant though for the description of the perfect reflection of a finite-amplitude Alfvén pulse.

This model is, of course, applicable not only to Gaussian-shaped pulses: functions of the form $1/(1+s^2)$ or $\mathrm{sech}^2 s$ produce qualitatively the same results.

The results obtained are important for a number of applications. The physical problem considered, namely the evolution of an initially static nonlinear Alfvén pulse, corresponds to a kinetic excitation of Alfvén waves by non-MHD forcing, which can take place in various astrophysical and laboratory situations. Also, the problem considered is very important for the interpretation of more sophisticated numerical simulations of initial value nonlinear MHD problems (see e.g. Nakariakov et al. 1997, 1998).

Acknowledgement

Erwin Verwichte acknowledges financial support by the Open University.

References

Allan, W. and Poulter, E. M. 1992 ULF waves – their relationship to the structure of the Earth's magnetosphere. *Rep. Prog. Phys.* **55**, 533–598.

Arber, T. D., Longbottom, A. W. and Van Der Linden, R. A. M. 1999 Unstable coronal loops: numerical simulations with predicted observational signatures. *Astrophys. J.* **517**, 990–1001.

Balogh, A., Smith, E. J., Tsurutani, B. T., Southwood, D. J., Forsyth, R. J. and Horbory, T. S. 1995 The heliospheric magnetic field over the south polar region of the Sun. *Science* **268**, 1007–1010.

Boynton, G. C. and Torkelsson, U. 1996 Dissipation of non-linear Alfvén waves. *Astron. Astrophys.* **308**, 299–308.

Cohen, R. H. and Kulsrud, R. M. 1974 Nonlinear evolution of parallel-propagating hydromagnetic waves. *Phys. Fluids* **17**, 2215–2225.

Minter, A. H. and Spangler, S. R. 1996 Observation of turbulent fluctuations in the interstellar plasma density and magnetic field on spatial scales of 0.01 to 100 parsecs. *Astrophys. J.* **458**, 194–214.

Nakariakov, V. M., Roberts, B. and Murawski, K. 1997 Alfvén wave phase mixing as a source of fast magnetosonic waves. *Solar Phys.* **175**, 93–105.

Nakariakov, V. M., Roberts, B. and Murawski, K. 1998 Nonlinear coupling of MHD waves in inhomogeneous steady flows. *Astron. Astrophys.* **332**, 795–804.

Rankin, R., Frycz, P., Tikhonchuk, V. T. and Samson, J. 1994 Nonlinear standing shear Alfvén waves in the Earth's magnetosphere. *J. Geophys. Res.* **99**, 21291–21301.

Spangler, S. R. 1997 Nonlinear evolution of MHD waves at the Earth's bow shock: opinions on the confrontations between theory, simulations, and measurements. In: *Nonlinear Waves and Chaos in Space Plasmas* (ed. T. Hada and H. Matsumoto), pp. 121–169. TERRAPUB, Tokyo.

Torkelsson, U. and Boynton, G. C. 1998 Non-linear spherical Alfvén waves. *Mon. Not. R. Astron. Soc.* **295**, 55–56.

Tikhonchuk, V. T., Rankin, R., Frycz, P. and Samson, J. C. 1995 Nonlinear dynamics of standing shear Alfvén waves. *Phys. Plasmas* **2**, 501–515.

Tsurutani, B. T., Thorne, R. M., Smith, E. J., Gosling, J. T. and Matsumoto, H. 1987 Steepened magnetosonic waves at comet Giacobini–Zinner. *J. Geophys. Res.* **92**, 11074–11082.

https://doi.org/10.1017/S0022377899007771 Published online by Cambridge University Press